SPE Brazil Flow Assurance Technology Congress
Rio de Janeiro, Brazil, November 15 – 18 2022

Experimental Investigation on Velocity Fields, Vorticity, and Turbulence within the Stage of an Electrical Submersible Pump (ESP)

Rodolfo M. Perissinotto[1*], William D.P. Fonseca[1], Rafael F.L. Cerqueira[2], William Monte Verde[2], Jorge L. Biazussi[2], Erick M. Franklin[1], Antonio C. Bannwart[1], Marcelo S. Castro[1]
[1]School of Mechanical Engineering - University of Campinas, UNICAMP, Brazil
[2]Center for Petroleum Studies - University of Campinas, UNICAMP, Brazil [*]rodolfomp@fem.unicamp.br

Abstract

This paper presents an experimental study on the flow dynamics within an Electrical Submersible Pump (ESP) stage. An ESP prototype with transparent impeller and diffuser was designed and manufactured to allow flow visualization, which was achieved by using a Time-Resolved Particle Image Velocimetry (TR-PIV) system. Single-phase water flow tests were conducted in various flow rates corresponding to percentages of the Best Efficiency Point (BEP). The average velocity fields, vorticity contours, and turbulent kinetic energy values obtained in the whole impeller reveal that the flow behaviour is very dependent on the ESP operational condition. Energy losses due to turbulence are lower when the pump works at the BEP. But when the device operates at off-design conditions, the flow becomes complex, with high vorticity and turbulence which cause a reduction in the performance. This type of investigation may be useful to validate numerical simulations, support the proposition of mathematical models, or help create improved impeller designs.

Keywords

Fluid Mechanics; Electrical Submersible Pump; Energy Losses.

Introduction

The Electrical Submersible Pump (ESP) is a device used as a relevant artificial lift method in the petroleum industry. However, when the ESP operates at conditions different from the Best Efficiency Point (BEP), it often experiences a decrease in its performance. In presence of viscous fluids or multiphase flows, there is frequently the occurrence of operational instabilities that may result in financial losses to the oil producers as well.

There is a clear dependence between the ESP behavior and the flow pattern in its stages. Therefore, researchers worldwide have been using flow visualization methods to improve the understanding on how the characteristics of the flow affect the functioning of the pump.

Examples of works focusing on single-phase flows in pumps include Pedersen et al. [1], Krause et al. [2], Keller et al. [3], Li et al. [4], Liu et al. [5]. The authors used the Particle Image Velocimetry (PIV) method in their investigations. In addition, other authors visualized two-phase flows within pumps with High-Speed Imaging (HSI) methods. We can cite Monte Verde et al. [6] and Perissinotto et al. [7] as examples, as they studied air-water and oil-water mixtures.

Flow visualization techniques have actually proven to be a powerful way to investigate these flows [8]. However, the use of visualization practices in ESPs is still a developing topic. In this context, this paper presents an experimental study on the flow inside the stage of a transparent pump, by using a Time-Resolved PIV (TR-PIV) technique.

Methodology

A new apparatus was designed and assembled to enable the visualization tests. It is composed of a water flow line with a tank, a booster pump, and instruments to measure the flow rate, pressure and temperature. In addition, the new test facility has a transparent ESP prototype which was especially developed for flow visualization purposes.

The prototype has an impeller whose geometry is based on a real ESP model P23, series 538, from *Baker Hughes*. A photo of the prototype stage, with the impeller and volute diffuser, is shown in Fig.1.

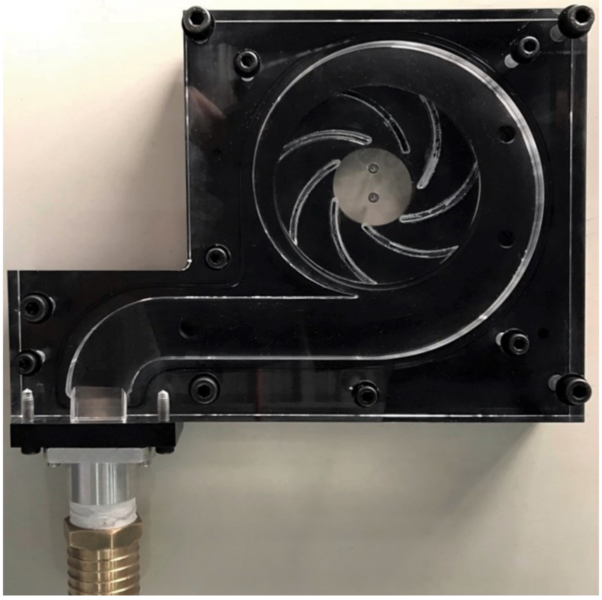

Figure 1. ESP prototype with transparent parts.

A TR-PIV system, *DualPower 30-1000* model, from *Dantec Dynamics*, was adopted here as the flow visualization method. This system provides up to a 30 mJ energy per pulse when operating at 1000 Hz repetition rate. Fluorescent PMMA particles doped with rhodamine were added to the water to work as tracers.

Experiments

The experiments were performed at five conditions by varying the water flow rates (Q) at fractions or multiples of the flow rate corresponding to the BEP (Q_{BEP}). The impeller rotational speed was kept at a constant value of $N = 900$ rpm. Table 1 lists all the operational points analysed in the present paper.

Table 1. Test matrix with five conditions.

Experimental condition at $N = 900$ rpm	Water flow rate relative to the BEP
1) $Q = 0.2\ m^3/h$	$Q = 0.1\ Q_{BEP}$
2) $Q = 1.8\ m^3/h$	$Q = 0.8\ Q_{BEP}$
3) $Q = 2.2\ m^3/h$	$Q = 1.0\ Q_{BEP}$
4) $Q = 2.6\ m^3/h$	$Q = 1.2\ Q_{BEP}$
5) $Q = 3.6\ m^3/h$	$Q = 1.6\ Q_{BEP}$

Each experiment consists of capturing 500 pairs of images using the *Dynamic Studio* software with the impeller at a fixed angular position measured by a rotational encoder. Such procedure ensures that all the channels and blades are always at the same position on the set of images, independently of the number of revolutions completed by the impeller.

Calculations

The images are then processed using algorithms in *MatLab*® and *Python*™ languages. A mask is firstly applied on the images in order to define the region of interest. When the impeller is analysed, the angular displacement between each pair of frames must be removed, so the relative velocity (u) can be obtained without considering the angular term. However, when the interest is directed to the entire stage, the angular term, proportional to the angular velocity (ω) and the radius (r), must be added to u. An absolute velocity (U) is thus found, as follows:

$$U = u + \omega r \qquad (1)$$

The velocities U and u displayed in Eq. (1) provide the average velocity fields within the ESP stage. By calculating the derivatives of these velocities, we can also estimate the vorticity intensity (ω_z):

$$\omega_z = \partial u_y / \partial x - \partial u_x / \partial y \qquad (2)$$

Furthermore, the variances of temporal fluctuations of the velocities ($\bar{u}'$) obtained from the PIV tests can help evaluate the Turbulent Kinetic Energy (k), or TKE, in the ESP stage:

$$k = [(\bar{u}_x')^2 + (\bar{u}_y')^2]/2 \qquad (3)$$

Results and Discussion

The vectors displayed in Figs. 2 to 4 represent the average relative velocity field at three different conditions. The impeller rotates clockwise.

Figure 2. Velocity field at $Q = 0.1\ Q_{BEP}$.

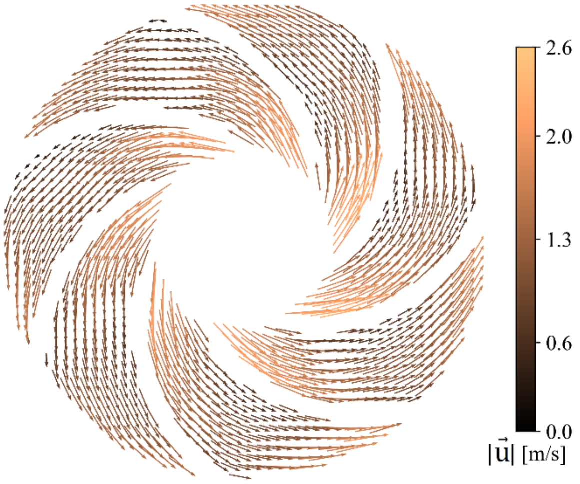

Figure 3. Velocity field at $Q = 1.0\ Q_{BEP}$.

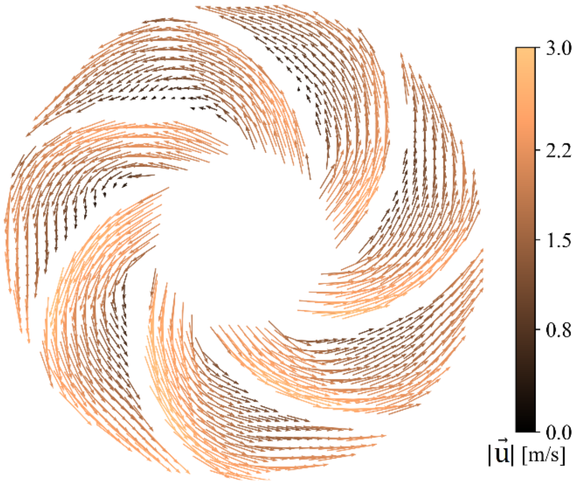

Figure 4. Velocity field at $Q = 1.6\ Q_{BEP}$.

As can be observed, the magnitudes of the velocity vectors are proportional to the water flow rate.

At the lowest flow rate, next to the shut-off condition (Fig. 2), the flow is very complex, full of vortices and regions of intense recirculation. These vortices are an effect of the adverse pressure gradient and flow separation caused by the blade tip [3]. The results agree with the observations made by other authors [1, 2, 4] in single-phase flows.

At the BEP (Fig. 3), the flow is more uniform. The vectors and streamlines are aligned with the blade curvature. In this condition, the energy losses in the pump are expected to be lower, so the efficiency is higher [1, 3].

At the highest water flow rate, next to the open-flow condition (Fig. 4), velocity vectors and streamlines undergo a deviation to the suction blades. The fluid path gets longer and the boundary layer detaches from the pressure blades [3]. The general structure of the flow is comparable to half a large vortex that rotates counterclockwise.

The contour plots of Fig. 5 show the vorticity in the impeller calculated from relative velocities. As can be noted, the regions with higher vorticity coincide with the position of the vortices at the shut-off, and the pressure blades at the open-flow.

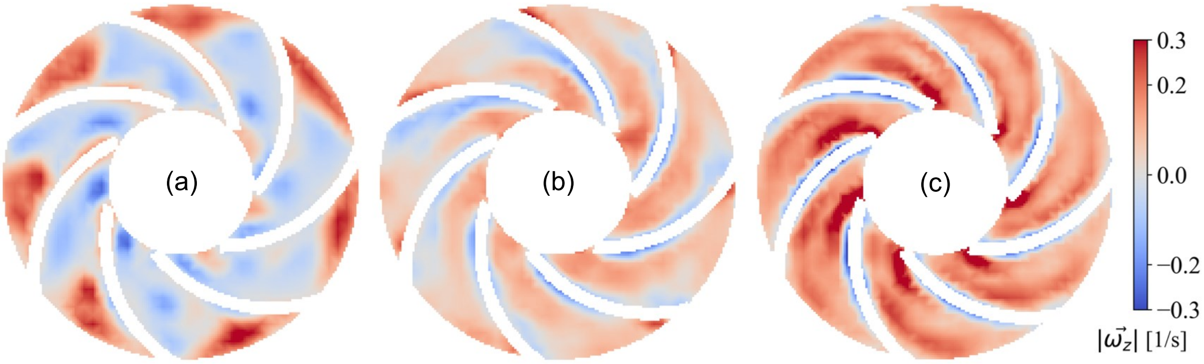

Figure 5. Contour plots of the vorticity in the impeller at (a) $Q = 0.1\ Q_{BEP}$, (b) $Q = 1.0\ Q_{BEP}$, (c) $Q = 1.6\ Q_{BEP}$.

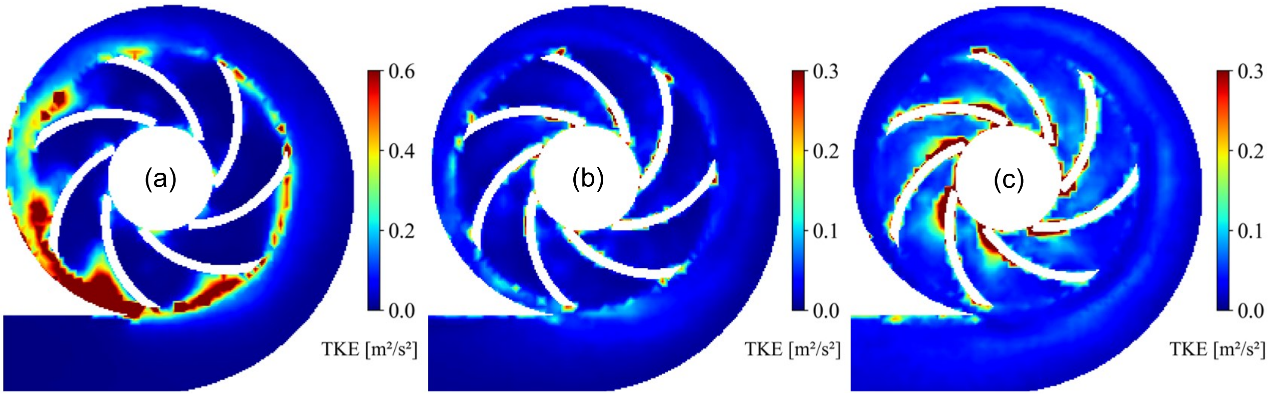

Figure 6. Contour plots of the turbulent kinetic energy at (a) $Q = 0.1\ Q_{BEP}$, (b) $Q = 1.0\ Q_{BEP}$, (c) $Q = 1.6\ Q_{BEP}$.

The contour plots of Fig. 6 contain the turbulent kinetic energy at the same three flow conditions. The highest TKE values are detected at the shut-off and open-flow points, where the energy losses are expected to be the highest. On the other hand, the Q_{BEP} has the lowest TKE and lowest energy losses, which are associated with a more efficient operation of the centrifugal pump.

To assess the total energy losses due to turbulence in the impeller as a whole, the TKE values at each impeller position were summed through numerical integration. Therefore, the total TKE (k_{sum}) was obtained and results are available in Fig. 7 for the five conditions listed in Table 1.

As can be observed, the value of k_{sum} is three times greater at the shut-off and open-flow points than at the conditions close to the BEP. Besides, the behavior of turbulence as a function of flow rate is represented by a second-degree polynomial fit, which has a coefficient of determination $R^2 = 0.98$.

The minimum value of the parabola occurs around $Q = 2.0\ m^3/h$, which corresponds to 90% of Q_{BEP}.

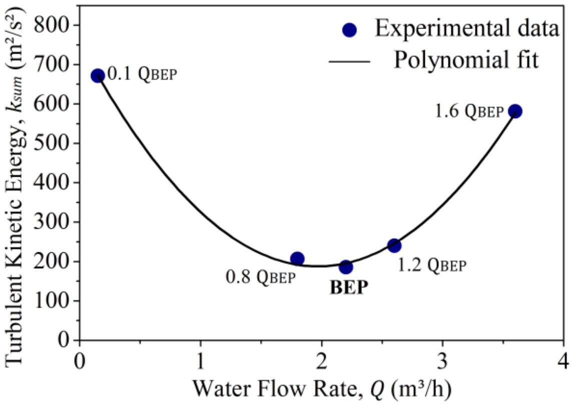

Figure 7. Total turbulent kinetic energy in the impeller at different flow rates (points) and a second-degree polynomial fit (curve).

Conclusions

In this work, the flow inside the single stage of a transparent pump was studied by using the TR-PIV approach. An experimental facility was designed and assembled for this analysis. This test section consists of transparent parts that provide a visual access to the flow inside the impeller and volute, in the entire stage, simultaneously. A set of five tests were executed by varying the water flow rates (i.e., $0.1\ \mathrm{Q_{BEP}} \leq \mathrm{Q} \leq 1.6\ \mathrm{Q_{BEP}}$), while maintaining the impeller rotational speed ($\mathrm{N} = 900\mathrm{rpm}$).

The acquisitions were performed at a fixed angular position defined by an encoder. The instantaneous PIV results were averaged for each experimental condition, resulting in the ensemble-averaged and turbulence statistics fields of the water flow in the ESP impeller. The average results reveal that the flow pattern changes as the flow rate deviates from the BEP condition.

For low Q values, the ensemble-averaged velocity fields indicate that the flow is full of vortices and regions of intense recirculation. As the flow rate increases, the flow gradually changes its pattern, becoming more uniform near the BEP, with velocity vectors aligned with the curvature of the blades. Then, from the BEP onwards, at high Q values, the velocity vectors undergo a deviation toward the suction blade direction.

In addition to the average velocity fields, the TKE contours in the different experimental conditions were also analyzed. As the operational point gets further from the BEP, the higher is the magnitude of the values. The TKE can be understood as the representation of the turbulence intensity in the impeller channels. Hence, the analysis of such fields, together with the time-resolved velocity data from the TR-PIV, may drive towards a more satisfactory understanding and math modeling of energy losses within the ESP.

The next steps of this study include, for example, extending the test matrix to assess other rotational speeds. In the near future, the turbulent dissipation rates will be estimated from another experimental program, together with other interesting quantities which depend on the instantaneous velocities.

Acknowledgments

We gratefully acknowledge the support of EPIC - Energy Production Innovation Center, hosted by the University of Campinas (UNICAMP) and sponsored by Equinor Brazil and FAPESP – The Sao Paulo Research Foundation (Process Number 2017/15736-3). We thank FAPESP for providing the PIV system used in this research through the Multi-User Equipment program (Process Number 2019/20870-6). We acknowledge the support of ANP (Brazil's National Oil, Natural Gas and Biofuels Agency) through the R&D levy regulation. The acknowledgments are also extended to the Center for Petroleum Studies (CEPETRO), School of Mechanical Engineering (FEM), and ALFA Research Group.

Responsibility Notice

The authors are the only responsible for the paper content.

References

[1] Pedersen, N.; Larsen, P.S.; Jacobsen, C.B. Flow in a centrifugal pump impeller at design and off-design conditions - Part I: particle image velocimetry (PIV) and laser doppler velocimetry (LDV) measurements. J. Fluids Eng. 2003, 125, pp. 61–72.

[2] Krause, N.; Pap, E.; Thévenin, D. Investigation of off-design conditions in a radial pump by using time-resolved-PIV. Proceedings of the 13th Int Symp on Applications of Laser Techniques to Fluid Mechanics, Lisbon, Portugal, 2006.

[3] Keller, J.; Blanco, E.; Barrio, R.; Parrondo, J. PIV measurements of the unsteady flow structures in a volute centrifugal pump at a high flow rate. Exp. Fluids 2014, 55, 1820.

[4] Li, X.; Chen, B.; Luo, X.; Zhu, Z. Effects of flow pattern on hydraulic performance and energy conversion characterization in a centrifugal pump. Renew. Energy 2020, 151, pp. 475–487.

[5] Liu, X-D.; Liu, Z-Q.; Zhong, Q.; Li, Y-J.; Yang, W. Experimental investigation of relative velocity field based on image rotation method in pump impeller. Flow Meas. Instrum. 2021, 82, 102061.

[6] Monte Verde, W.; Biazussi, J.L.; Sassim, N.A.; Bannwart, A.C. Experimental study of gas-liquid two-phase flow patterns within centrifugal pumps impellers. Exp. Therm. Fluid Sci. 2017, 85, pp. 37–51.

[7] Perissinotto, R.M.; Monte Verde, W.; Gallassi, M.; Gonçalves, G.F.N.; Castro, M.S.; Carneiro, J.; Biazussi, J.L.; Bannwart, A.C. Experimental and numerical study of oil drop motion within an ESP impeller. J. Petrol. Sci. Eng. 2019, 175, pp. 881–895.

[8] Perissinotto, R. M.; Monte Verde, W.; Biazussi, J. L.; Bulgarelli, N. A. V.; Fonseca, W. D. P.; Castro, M. S.; Franklin, E. M.; Bannwart, A. C. Flow visualization in centrifugal pumps: A review of methods and experimental studies. J. Petrol. Sci. Eng. 2021, 203, 108582.